Journal Pre-proofs

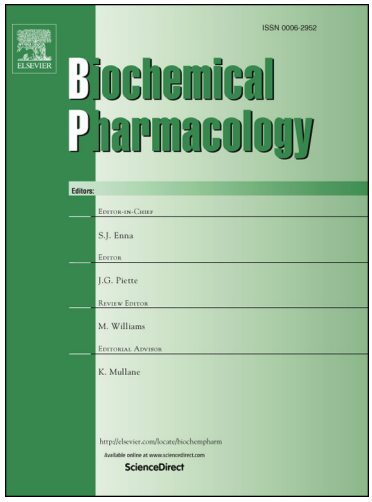

Thrombin/PAR-1 activation induces endothelial damages via NLRP1 inflammasome in gestational diabetes

Yue Liu, Zhuang-Zhuang Tang, Yu-Meng Zhang, Li Kong, Wei-Fen Xiao, Teng-Fei Ma, Yao-Wu Liu

PII: S0006-2952(20)30070-8
DOI: https://doi.org/10.1016/j.bcp.2020.113849
Reference: BCP 113849

To appear in: *Biochemical Pharmacology*

Received Date: 15 December 2019
Accepted Date: 6 February 2020

Please cite this article as: Y. Liu, Z-Z. Tang, Y-M. Zhang, L. Kong, W-F. Xiao, T-F. Ma, Y-W. Liu, Thrombin/PAR-1 activation induces endothelial damages via NLRP1 inflammasome in gestational diabetes, *Biochemical Pharmacology* (2020), doi: https://doi.org/10.1016/j.bcp.2020.113849

This is a PDF file of an article that has undergone enhancements after acceptance, such as the addition of a cover page and metadata, and formatting for readability, but it is not yet the definitive version of record. This version will undergo additional copyediting, typesetting and review before it is published in its final form, but we are providing this version to give early visibility of the article. Please note that, during the production process, errors may be discovered which could affect the content, and all legal disclaimers that apply to the journal pertain.

© 2020 Published by Elsevier Inc.

Journal Pre-proofs

Thrombin/PAR-1 activation induces endothelial damages via NLRP1 inflammasome in gestational diabetes

Yue Liu[a], Zhuang-Zhuang Tang[a], Yu-Meng Zhang[a], Li Kong[a], Wei-Fen Xiao[b], Teng-Fei Ma[c], Yao-Wu Liu[a,d,*]

[a]*Jiangsu Key Laboratory of New Drug Research and Clinical Pharmacy, Xuzhou Medical University, Xuzhou 221004, Jiangsu, China*

[b]*Department of Obstetrics and Gynecology, Xuzhou Medical University Affiliated Hospital, Xuzhou 221006, Jiangsu, China*

[c]*Key Laboratory of Targeted Intervention of Cardiovascular Disease, Collaborative Innovation Center for Cardiovascular Disease Translational Medicine, Nanjing Medical University, Nanjing 211166, Jiangsu, China*

[d]*Department of Pharmacology, School of Pharmacy, Xuzhou Medical University, Xuzhou 221004, Jiangsu, China*

*Corresponding author: Yao-Wu Liu

Jiangsu Key Laboratory of New Drug Research and Clinical Pharmacy, Xuzhou Medical University

No. 209, Tongshan Road, Xuzhou 221004, Jiangsu, China

ywliu@xzhmu.edu.cn (Liu YW)

Tel: +86-516-83262107

Fax: +86-516-83262630

Running Head: Thrombin/PAR-1 mediated endothelial damages in GDM

Abbreviations

AGEs	advanced glycation endproducts
AG	aminoguanidine
Arg	argathroban
DM	diabetes mellitus
ELISA	enzyme-linked immunosorbent assay
HG	high glucose
HUVECs	human umbilical vein endothelial cells
IL	interleukin
GDM	gestational diabetes mellitus
LDH	lactate dehydrogenase
NLRP1	nucleotide-binding domain and leucine-rich repeat containing protein 1
PAR-1	protease-activated receptor 1
qPCR	real-time fluorescence quantitative PCR
RAGE	receptor for advanced glycation endproducts
Sar	sarsasapogenin
shRNA	short hairpin RNA
Vor	vorapaxar

Journal Pre-proofs

Abstract

Gestational diabetes mellitus (GDM) is associated with an increased risk of progressing to type 2 DM and cardiovascular disease; however, the pathogenesis is still poorly understood. This study was to investigate roles of thrombin and its receptor protease-activated receptor 1 (PAR-1) and NLRP1 inflammasome in endothelial injury in GDM condition. Umbilical cord and plasma of GDM patients and high glucose (HG) cultured human umbilical vein endothelial cells (HUVECs) were used to examine the pathological changes of these pathways. Meanwhile, ameliorative effects and potential mechanisms of a natural product sarsasapogenin (Sar) were investigated in HUVECs. Thrombin/PAR-1 pathway, advanced glycation endproducts (AGEs) and their receptor (RAGE) axis, and the nucleotide-binding domain and leucine-rich repeat containing protein 1 (NLRP1) inflammasome were activated in GDM condition and HG-cultured HUVECs, accompanied by endothelial injury (decreased cell viability and increased lactate dehydrogenase release). Nevertheless, thrombin inhibition or PAR-1 antagonism caused decreases in AGEs formation and RAGE expression in HG-cultured HUVECs, while AGEs inhibition or RAGE antagonism declined PAR-1 expression not thrombin activity. Furthermore, thrombin inhibition or PAR-1 antagonism restrained NLRP1 inflammasome activation in HG-cultured HUVECs; meanwhile, NLRP1 expression and interleukin 18 levels were remarkably reduced in HG-cultured HUVECs after PAR-1 knockdown. Interestingly, Sar co-treatment could suppress thrombin/PAR-1 pathway, NLRP1 inflammasome, and AGEs/RAGE axis. Together, endothelial damages in GDM were likely due to enhanced interaction between AGEs/RAGE axis and thrombin/PAR-1 pathway, followed by NLRP1 inflammasome activation. Moreover, Sar may act as a protective agent against endothelial injury in chronic HG condition.

Key words: Gestational diabetes mellitus; endothelial injury; thrombin/PAR-1 pathway; NLRP1 inflammasome; AGEs/RAGE axis; sarsasapogenin

Journal Pre-proofs

1. Introduction

Gestational diabetes mellitus (GDM) is a disease of abnormal glucose tolerance during pregnancy, which is accompanied by a series of adverse responses in pregnant women [1], subsequently leading to fetal macrosomia, respiratory distress syndrome, and type 2 diabetes in the offspring [2]. Although abnormal glucose tolerance usually returns to normal in the immediate postpartum period, women with GDM have a 20-70% risk of progressing to type 2 diabetes in the first decade after delivery [3]. However, at present, the mechanisms of how GDM develops type 2 diabetes are still unclear. Thus, it is important to deeply clarify the biochemical pathways in GDM. Moreover, pharmacological interventions might prevent or delay the onset of type 2 diabetes in the affected women.

Physiological changes of blood coagulation occur and might be at a prethrombotic state in normal pregnancy, especially in middle and late stages [4]. Simultaneously patients with diabetes are in a systemic and chronic blood hypercoagulability condition due to hypercoagulation and platelet activation [5]. Therefore, GDM may aggravate the changes of blood coagulation in normal pregnancy [6, 7]. Thrombin, a serine protease produced during intravascular coagulation, is typically regarded as a consequence of vascular injury, and protease-activated receptors (PARs) mediate the effects of thrombin in normal and disease states [8]. Vascular endothelial injury and chronic low-grade inflammation have been considered central points in the pathophysiology of GDM [9-11]. Elevated levels of inflammatory mediators may be associated with an increased coagulability and a tendency towards thrombus formation in patients with type 2 diabetes who have microvascular complications [12], suggesting an interaction between inflammation and blood coagulation system [5]. Thrombin and PAR-1, a prototypical receptor of thrombin, also play

important roles in vascular physiology and inflammation [13-15]. Ishibashi et al. report that advanced glycation endproducts (AGEs), key factors for diabetic complications in microangiopathy, potentiate the citrated plasma-induced oxidative and inflammatory reactions in endothelial cells via the activation of thrombin/PAR-1 system [16]. Early reports show that proinflammatory effect of thrombin and PAR-1 is associated with NF-kappaB activation [17, 18], while interleukin 1β (IL-1β) enhances granzyme B-mediated neurotoxicity by increasing PAR-1 expression [19]. Moreover, a recent report indicates that high glucose induced endothelial injury is associated with NLRP3 inflammasome activation in human umbilical vein endothelial cells (HUVECs) [20]. Thus, inflammatory responses caused by thrombin/PAR-1 pathway may involve the activation of NLRP3/1 inflammasome besides NF-kappaB activation in endothelium. However, it is not clear about the role of thrombin and PAR-1 signaling in high glucose-caused endothelial damages in GDM condition, and the relationship of thrombin/PAR-1 pathway and NLRP1 inflammasome activation is not understood in vascular endothelial cells.

Sarsasapogenin (Sar) is a major steroidal sapogenin of the timosaponins separated from the Chinese Materia Medica *Rhizoma Anemarrhenae* (family Asparagaceae). Timosaponin AIII and BII, the common glycosides of Sar, are reported to show significant antiplatelet, antithrombotic effects and anti-inflammatory actions [21, 22], indicating that timosaponins and the major aglycon Sar have anticoagulation and antithrombotic effects [23-25]. Importantly, timosaponin AIII and Sar ameliorate colitis in mice, and the vitro and in vivo anti-inflammatory effects of Sar are more potent than AIII [26]. In addition, a recent report from our team showed that Sar markedly ameliorated diabetic nephropathy in rats via inhibiting NLRP3 inflammasome activation and AGEs/RAGE interaction [27]. Thus, anti-inflammatory effects may contribute to the

anticoagulation and antithrombotic effects of timosaponins and Sar, and Sar may be a good candidate for protection of the vascular endothelium.

In this study, our aims were: firstly, whether thrombin/PAR-1 pathway and the NLRP1 inflammasome were activated in GDM patients and HUVECs cultured with high glucose; secondly, whether activated thrombin/PAR-1 resulted in the activation of NLRP1 inflammasome; thirdly, whether enhanced AGEs/RAGE interaction mediated the activated thrombin/PAR-1 signaling in HUVECs in high glucose condition; finally, whether a natural compound Sar ameliorated the damaged vascular endothelium in high glucose-cultured HUVECs.

2. Materials and Methods

2.1. Human specimen collection

GDM was diagnosed according to the International Association of the Diabetes and Pregnancy Study Group (IADPSG) criteria: The pregnant women with 24-28 weeks were subjected to oral glucose tolerance test by using 75 g glucose; then those patients were diagnosed to GDM with any of the following results: fasting plasma glucose $\geqslant$ 5.1 mmol/L, 1 h plasma glucose $\geqslant$ 10.0 mmol/L, and 2 h plasma glucose $\geqslant$ 8.5 mmol/L [28]. The high blood glucose in GDM patients was controlled using diet or insulin. For insulin control, the blood glucose was kept within 4.4 mmol/L after fasting or at 6.7 mmol/L for 2 hour post-meal. The umbilical cord tissues of pregnant women with and without GDM hospitalized in full-term pregnancy were collected in the cesarean section operating room of the Affiliated Hospital of Xuzhou Medical University. The umbilical cord tissue 2 to 3 cm near the fetus side was cut and collected, one part for paraffin embedding and the other part preserved in the -80°C refrigerator for use. Serum samples were collected from the Department of Clinical Laboratory of the Affiliated Hospital of Xuzhou

Medical University. The experiment obtained an approval from the Ethics Committee of the Affiliated Hospital of Xuzhou Medical University (reference number: XYFY2019-KL172-02).

2.2. HUVECs culture and treatments

The HUVECs cell line was purchased from Shanghai Bioengineering Biotechnology Co., Ltd, China. HUVECs cultured in vitro at passage 5 to 10 were used for experiments. The cells were cultured in Dulbecco's modified Eagle medium (DMEM) containing 10% fetal bovine serum. DMEM culture medium and fetal bovine serum were purchased from Hyclone (Logan, UT, USA). After incubation for 24 h under normal conditions (medium containing 5.56 mmol/L glucose, 10% FBS, 100 U/mL penicillin and 100 μg/mL streptomycin, 5% CO_2, 37 °C) and subsequent cell cycle synchronization for 12 h, HUVECs were divided into the following groups: normal glucose group (NG, 5.56 mmol/L glucose), high glucose group (HG, 30 mmol/L glucose), low, middle, and high concentrations of Sar group (HG+Sar, 30 mmol/L glucose plus 0.2, 1.0, 5.0 μmol/L sarsasapogenin, respectively), PAR-1 antagonist group (HG+Vor, 30 mmol/L glucose plus 1.0 μmol/L vorapaxar), thrombin inhibitor group (HG+Arg, 30 mmol/L glucose plus 1.0 μmol/L argatroban), AGEs inhibitor group (HG+AG, 30 mmol/L glucose plus 1.0 μmol/L aminoguanidine), and RAGE antagonist group (HG+FPS-ZM1, 30 mmol/L glucose plus 1.0 μmol/L FPS-ZM1). Sarsasapogenin (purity > 98%) was purchased from Beijing Medicass Biotechnologies, Co. Ltd., China, vorapaxar d from Selleckchem (Shanghai), argatroban from Sigma-Aldrich (Shanghai), aminoguanidine from Aladdin (Shanghai), and FPS-ZM1 from MedChemExpress (Shanghai), China. Sarsasapogenin and all the above tool drugs were dissolved in dimethylsulfoxide and made into stock solutions for use. After treatment with the above different agents for 48 h, the cells were harvested for indices analysis. The culture time was

156 selected according to the changes of PAR-1 protein in HUVECs cultured with 30 mmol/L glucose
157 for 24 h, 48 h, and 72 h, respectively.

158 2.3. PAR-1 knockdown in HUVECs

159 Lentivirus carrying F2R shRNA (shF2R) (Shanghai Genechem Gene Chemical Technology, Co.
160 Ltd., China) was transfected into HUVECs, establishing a stable cell line with PAR-1 knockdown.
161 After 72 h of screening with puromycin (Xuzhou VICMED Bioengineering Co., Ltd., China),
162 samples of cell stable strains were collected. Then the interference efficiency of shF2R was
163 confirmed, and the cells were divided into two kinds: negative control (shNC) and PAR-1
164 knockdown (shF2R). The specific groups were: HG group (30 mmol/L glucose), HG+Sar group
165 (30 mmol/L glucose plus 5 μmol/L Sar), shF2R+HG group (30 mmol/L glucose in shF2R cells),
166 and shF2R+HG+Sar, (30 mmol/L glucose plus 5 μmol/L in shF2R cells). The protein expression
167 of NLRP1 was detected by Western blot and intracellular IL-18 level by enzyme-linked
168 immunosorbent assay (ELISA).

169 2.4. CCK-8 assay for cell viability

170 CCK-8 assay was used for cell damage [29]. Briefly, cell suspension (100 μL/well, 1.0×10^6/ml)
171 was pre-incubated in a 96-well plate for 24-48 h at 37°C in a humidified atmosphere of 5% CO_2.
172 After the cells were incubated in different groups for 24 h, 10 μL of the CCK-8 solution (Dongren
173 Chemical Technology (Shanghai) Co. Ltd., China) was added to each well of the plate and
174 incubated for 2 h in incubator. After 10 μL of 1% (w/v) SDS added to each well in dark at room
175 temperature, the absorbance was determined at 450 nm using a microplate reader. The net
176 absorbance of the normal glucose group was considered as 100% of the cell viability.

177 2.5. Lactate dehydrogenase (LDH) release for cytotoxicity

LDH release was used to further assess endothelial cell injury referring to previous report [30]. Add 100 μL of cell suspension to each well in 96-well plate, mix and prepare in culture incubator (37 °C, 5% CO_2) for 24 h. One hour before the scheduled detection time point, the cell culture plate was taken out from the cell culture incubator, and the reagent provided by the LDH release kit (Beyotime Biotechnology, Nantong, China) was added to the "control well with maximum enzyme activity". After adding the reagents of LDH release, mix repeatedly and continue to incubate in the cell culture incubator. After the predetermined time was reached, the cell culture plates were centrifuged at 400 g for 5 min. Then 120 μL of the supernatant was taken and added to the corresponding well in a new 96-well plate, and then 60 μL of test solution of LDH release was added, mixed well, and incubated at room temperature for 30 min in the dark. The absorbance was then measured at 490 nm. The net absorbance of the normal glucose group was considered as 100% of the LDH release.

2.6. Determination of thrombin activity

Thrombin activity was measured by a fluorometric assay based on the cleavage rate of the synthetic thrombin substrate Boc-Asp (OBzl)-Pro-Arg-AMC according to previous study [31]. The protein concentration in the supernatant of tissues or cells was determined by the BCA method. Tris/HCL 1.21 g, $CaCl_2$ 22.2 mg, NaCl 1.755 g, and BSA 0.2 g were dissolved in 200 mL of deionized water (pH = 8.8) to prepare a buffer solution, which was stored at 4°C until use. The 77 mg Boc-Asp (OBzl)-Pro-Arg-AMC fluorogenic substrate (Nanjing Peptide Industry Biotechnology Co., Ltd, China) was dissolved in 10 mL of DMSO, and 1.0 mg bestatin (Selleckchem, Shanghai, China) in 1 mL DMSO, mixed well in dark, and stored at -20°C. According to protein amount of 60 μg, the enzymatic sample was added to the reaction system

with a final volume 100 μL including bestatin and the fluorescent substrate in a black 96-well microplate, and then fully mixed. The reaction was carried out in an oven at 37 °C for 50 min, and the optical density value was immediately measured with a fluorescence spectroscopy at the excitation wavelength 360 nm and emission wavelength 465 nm. The net absorbance from the plates of cells cultured with normal glucose was considered as 100% thrombin activity.

2.7. ELISA assay of IL-18 and IL-1β

IL-18 and IL-1β levels were measured by using corresponding human IL-18 and IL-1β ELISA kits (Wuhan Boster Bio-technology Co., Ltd., China) according to the manufacturer's instructions.

2.8. Western blotting analysis for PAR-1, cleaved-caspase-1, NLRP1, and RAGE levels

Protein concentration of the sample was determined using a BCA protein assay kit (Thermo Scientific, Rockford, IL, USA). The protein samples were separated using sodium dodecyl sulfate polyacrylamide gel electrophoresis and transferred to polyvinylidene fluoride membrane (Millipore, Bedford, MA, USA). The membrane was blocked with 2% milk powder solution for 60 min and incubated over night at 4°C with primary antibodies anti-β-actin (Bioworld Technology, Inc., St. Louis, USA, 1:1000), anti-RAGE (Abcam Company, Cambridge, UK, 1:1000), anti-PAR-1 (Sigma-Aldrich Company, Shanghai, China, 1:1000), anti-cleaved-caspase-1 (Bioworld Technology, Inc., Bloomington, USA, 1:1000), and anti-NLRP1 (Abcam Company, Cambridge, USA, 1:1000). The proteins were detected using goat anti rabbit IgG(H+L) secondary antibodies (Li-Cor Inc., Lincoln, NE), respectively. Infrared Imaging System (Gene Company Limited, Hong Kong, China) was applied to detect immunoreactive blots. The signal densities on the blots were measured with Image J software and normalized using rabbit anti-β-actin antibody (Bioworld Technology, St. Louis, USA) or rabbit anti-GAPDH antibody (ABclonal

Biotechnology Co., Ltd., Boston, USA) as an internal control.

2.9. Immunofluorescence analysis for PAR-1 and AGEs

Immunofluorescence assay was performed according to the report [32]. Cells plated on coverslips were fixed with 4% paraformaldehyde for 15 min, permeabilized with 0.1% TritonX-100 in PBS for 5 min, treated with blocking medium (1% bovine serum albumin in PBS) for 30 min, and then incubated with anti-PAR-1 antibody (Cat No.Cleaved-Ser42, Sigma-Aldrich Company, Shanghai, China) or anti-AGEs antibody (Abcam Company, Cambridge, UK), at 37°C for 2 h. Immune-reacted primary antibody was detected after 1-h incubation in dark place at 37°C with a secondary antibody Dylight 594 Affinipure donkey anti-rabbit IgG (H+L) (Earthox, Millbrae, CA, USA).The cells were further stained with DAPI (Vector, Burlingame, CA, USA) for 2 min in dark place at room temperature and washed, then mounted onto microscope slides in mounting medium. Observations were carried out by using an Olympus BX43F fluorescence microscope (Tokyo, Japan).

2.10. AGEs expression in umbilical cord by immunofluorescence

Protein detection in tissue paraffin section by immunofluorescence assay was conducted as our previous report [27]. Briefly, 4-μm sections were incubated with anti-AGEs antibody (Abcam Company, Cambridge, UK, 1:200) overnight at 4 °C followed by the secondary antibody Dylight 594-AffiniPure donkey anti-rabbit IgG(H+L) (EarthOx, LLC, Millbrae, USA). Then, the sections were further stained with DAPI (Vector, Burlingame, USA) for 3 min in dark place. Finally, the sections were examined using an Olympus BX43F fluorescence microscope (Tokyo, Japan).

2.11. Statistical analysis

All statistical analyses were carried out using GraphPad Prism 7.0 software. The values (a

maximum of two) with a large dispersion to the mean were rejected during data entry. An unpaired, two-tailed Student's t test was performed for statistical analysis or one-way ANOVA with Dunnet's post hoc tests for analysis, wherever applicable. Data were represented as mean ± SEM. A P value < 0.05 was considered statistically significant.

3. Results

3.1. Activation of the thrombin/PAR-1 pathway and AGEs/RAGE axis in GDM patients

To determine whether the thrombin/PAR-1 pathway was activated in GDM patients, thrombin activity and protein expression of PAR-1 were assessed in umbilical cord. The data indicated that enzymatic activity of thrombin and protein expression of PAR-1 were significantly (both P < 0.01) increased in the umbilical cord of GDM women, compared with those in normal pregnant women (Fig. 1A, B). Meanwhile, further to investigate the alteration of AGEs/RAGE axis in GDM condition, AGEs levels and protein expression of RAGE were determined in the GDM women. It was found that protein expression of RAGE (P < 0.01) as well as AGEs levels was markedly up-regulated in the umbilical cord of GDM women, compared with the normal pregnant women (Fig. 1C, D). These results indicated that both thrombin/PAR-1 pathway and AGEs/RAGE axis were activated in vascular endothelium in GDM condition.

3.2. Activation of the NLRP1 inflammasome in GDM patients

In order to explore whether activation of the NLRP1 inflammasome occurred in GDM patients, protein expression of NLRP1 and cleaved-caspase 1 (two major components of the NLRP1 inflammasome) in umbilical cord, and an important product IL-18 levels in plasma were examined. GDM significantly (P < 0.05 or P < 0.01) raised the protein expressions of NLRP1 and cleaved-caspase 1 in umbilical cord as well as IL-18 levels in plasma of the expectant women,

compared with the normal expectant mothers (Fig. 2A, B, C). However, it was found that IL-1β levels were very low in plasma of GDM patients (data not shown). So the NLRP1 inflammasome was activated in GDM condition.

3.3. Activation of the thrombin/PAR-1 pathway in HG-cultured HUVECs and effects of Sar

To thoroughly investigate the changes of those pathways in GDM condition, HG-cultured HUVECs (a cell line of endotheliocyte) was used. Protein expression of PAR-1 was selected to be examined in HUVECs cultured with high glucose for different time to seek for applicable culture protocol. It was found that 30 mmol/L glucose obviously increased the protein expression of PAR-1 in HUVECs after culture for both 48 h and 72 h by immunofluorescence analysis, while PAR-1 protein was slightly raised for 24 h culture (Fig. 3). So the in vitro experiment protocol HUVECs cultured with 30 mmol/L glucose for 48 h was adopted.

Chronic HG culture moderately increased thrombin activity in HUVECs compared with normal glucose group (Fig. 4A), while dramatically ($P < 0.05$) up-regulated PAR-1 protein expression (Fig. 4B). The results were similar to those in GDM patients (Fig. 1A, B). Nonetheless, both PAR-1 antagonism with vorapaxar and thrombin inhibition with argatroban reversed the increase in PAR-1 protein expression in HG-cultured HUVECs (Fig. 4B), verifying a vital role of PAR-1 in vascular endothelial functions. Furthermore, treatment with a natural compound Sar significantly ($P < 0.05$ or $P < 0.01$) declined thrombin activity and PAR-1 protein expression at both 1.0 and 5.0 μmol/L in HG-cultured HUVECs (Fig. 4A, B), demonstrating that Sar could suppress thrombin/PAR-1 pathway.

3.4. Activation of AGEs/RAGE axis in HG-cultured HUVECs and effects of Sar

The formation of AGEs and protein expression of RAGE were also investigated in HG-cultured

HUVECs to seek for the potential mechanism of the activated thrombin/PAR-1 pathway. Immunofluorescence study demonstrated that AGEs level was markedly increased in HG-cultured HUVECs (Fig. 5A), and protein expression of RAGE was also remarkably ($P < 0.01$) up-regulated in HUVECs exposed to chronic HG (Fig. 5B). However, both the AGEs levels and RAGE expression were significantly ($P < 0.05$ or $P < 0.01$) decreased in all three concentrations of Sar groups, compared to the untreated groups in HG-cultured HUVECs (Fig. 5A, B), suggesting a strong inhibitory effect of Sar on AGEs/RAGE interaction.

3.5. Endothelial injury in HG-cultured HUVECs and effects of Sar

In order to examine whether the activated thrombin/PAR-1 pathway resulted in vascular endothelial injury in prolonged HG condition, cell viability and LDH release were detected in HG-cultured HUVECs. Figure 6A showed that cell viability was markedly ($P < 0.05$) decreased in HUVECs cultured with HG for 48 h related to that in HUVECs cultured with normal glucose, and LDH release was remarkably ($P < 0.01$) promoted in HG-cultured HUVECs (Fig. 6B). Nonetheless, a PAR-1 antagonist or a thrombin inhibitor significantly ($P < 0.05$ or $P < 0.01$) reduced LDH release in HG-cultured HUVECs, and the effect of PAR-1 antagonism was better than that of thrombin inhibition (Fig. 6B). These reflected a contribution of the thrombin/PAR-1 pathway to vascular endothelial injury under the high glucose conditions. Moreover, cell viability and LDH release were significantly ($P < 0.05$ or $P < 0.01$) ameliorated by Sar at the concentrations of 0.2, 1.0, and 5.0 μmol/L in HG-cultured HUVECs (Fig. 6A, B).

3.6. Activation of the NLRP1 inflammasome in HG-cultured HUVECs and effects of Sar

In order to explore whether the NLRP1 inflammasome was activated in HUVECs exposed to chronic HG, protein expressions of NLRP1 and cleaved-caspase 1 as well as the levels of IL-18

and IL-1β were determined. Results indicated that NLRP1 inflammasome was significantly activated in HG-cultured HUVECs, as evidenced by the increased protein expressions of NLRP1 ($P < 0.01$) and cleaved-caspase 1 ($P < 0.05$), and the elevated levels of IL-18 and IL-1β (both $P < 0.01$), compared with the culture with normal glucose (Fig. 7A-D). Moreover, treatment with Sar at 1.0 or 5.0 μmol/L had similar ameliorative effects to thrombin/PAR-1 pathway inhibition on the activation of NLRP1 inflammasome in HG-cultured HUVECs, while 0.2 μmol/L Sar mildly improved these indices (Fig. 7A-D). Together with our previous report [27], we could conclude Sar indeed had an inhibitory efficacy on NLRP1/3 inflammasome.

3.7. Interaction between AGEs/RAGE axis and thrombin/PAR-1 pathway in HG-cultured HUVECs

To verify whether the activated thrombin/PAR-1 pathway was associated with the enhanced AGEs/RAGE interaction in HG-cultured HUVECs, both thrombin activity and PAR-1 expression were assessed in the presence and absence of AGEs inhibition or RAGE antagonism. It was found that protein expression of PAR-1 was markedly (both $P < 0.01$) reduced in HUVECs co-cultured with HG plus either aminoguanidine (AG, a typical inhibitor of AGEs formation) or FPS-ZM1 (a high-affinity antagonist of RAGE) (Fig. 8A), as well as co-culture with HG and high concentration of Sar (Fig. 8A). However, thrombin activity was not changed in HUVECs co-cultured with HG plus either aminoguanidine or FPS-ZM1, compared with HG culture alone (Fig. 8B), but thrombin activity was still significantly ($P < 0.05$) decreased after co-culture with HG and high concentration of Sar (Fig. 8B). These results demonstrated that it was thrombin receptor PAR-1 not thrombin itself that was influenced by AGEs/RAGE axis in HUVECs in HG condition. On the other hand, high glucose co-culture with a thrombin inhibitor argatroban or a

PAR-1 antagonist vorapaxar markedly attenuated the increase in AGEs level in HUVECs (Fig. 5A), and greatly ($P < 0.05$ or $P < 0.01$) suppressed the expression of RAGE (Fig. 5B), compared with HG culture alone. Taken together, a crosstalk may exist between thrombin/PAR-1 pathway and AGEs/RAGE axis in vascular endothelial injury in high glucose condition.

3.8 Thrombin/PAR-1 pathway mediated the activation of NLRP1 inflammasome in HG-cultured HUVECs

The mechanism of the proinflammatory effect of activated thrombin/PAR-1 pathway was explored from the point of NLRP1 inflammasome activation in HG-cultured HUVECs. Compared with high glucose culture alone, high glucose co-culture with a thrombin inhibitor argatroban or a PAR-1 antagonist vorapaxar reversed the increases in NLRP1, cleaved-caspase 1, IL-18, and IL-1β levels in HG-cultured HUVECs (Fig. 7A-D), showing that activated thrombin/PAR-1 pathway may cause NLRP1 inflammasome activation in HG-cultured HUVECs. To further testify this relationship, a HUVEC line with a stable PAR-1 knockdown by using short hairpin RNA (shRNA) was established. The interference efficiency of F2R shRNA (F2R as the gene symbol of PAR-1) (Fig. 9) was enough to perform the following experiment. It was found that NLRP1 and IL-18 levels were dramatically (both $P < 0.01$) decreased in HG-cultured HUVECs with PAR-1 knockdown, compared to those in HG-cultured HUVECs with normal PAR-1 expression (Fig. 10A, B). The similar results were obtained by using HG co-treatment with high concentration of Sar (i.e. HG+Sar-5) in the condition of PAR-1 knockdown (Fig. 10A, B). Altogether, we could obtain that the proinflammatory effect of activated thrombin/PAR-1 pathway was achieved through the activation of NLRP1 inflammasome in vascular endothelium in high glucose condition.

4. Discussion

In this study, we found that thrombin/PAR-1 pathway, the NLRP1 inflammasome, and AGEs/RAGE axis were activated in the umbilical cord of GDM patients. In HUVECs cultured with chronic high glucose, the above mentioned pathways were also activated, in couple with noteworthy endothelial injuries. Further studies demonstrated that there may be a crosstalk between AGEs/RAGE axis and thrombin/PAR-1 pathway, followed by the activation of NLRP1 inflammasome in HG-cultured HUVECs. Moreover, a natural compound sarsasapogenin ameliorated endothelial damages caused by chronic high glucose, which was achieved through suppressing vascular inflammation mediated by both AGEs/RAGE axis and thrombin/PAR-1 pathway.

The physiological changes of blood coagulation occur in normal pregnancy and might be at a prethrombotic state, evidenced by both the increased coagulation activity and the reduced anticoagulation and fibrinolytic activity [4]. Gumus et al. reported that thrombin-activatable fibrinolysis inhibitor antigen levels in plasma were significantly higher in pregnant women with GDM when compared with controls, and may contribute to the decreased fibrinolytic potency, causing a thrombophilic state [7]. The present study indicated that thrombin activity was markedly elevated in the umbilical cord of GDM patients and HG-cultured HUVECs. Furthermore, protein expression of PAR-1 was significantly raised in both the umbilical cord of GDM patients and HG-cultured HUVECs, indicating that thrombin/PAR-1 pathway was activated in the vascular endothelial cells in GDM condition.

Obvious vascular endothelial injury happens in GDM condition, which is closely related to inflammation [11]. Accumulating data suggest that inflammasomes, mainly NLRP3 and NLRP1,

376 are involved in the generation of tissue or organ damage through exaggerating systemic and
377 organ-specific inflammatory responses [33]. We found that the NLRP1 inflammasome was
378 activated in GDM patients, for protein expressions of its main components NLRP1 and
379 cleaved-caspase 1 in the umbilical cord and its product IL-18 levels in plasma were remarkably
380 elevated. Similarly, the NLRP1 inflammasome was also activated in HG-cultured HUVECs,
381 accompanied by the damaged endothelial functions. Additionally, Jiang et al. reported that the
382 NLRP3 inflammasome activation was also involved in HG-induced endothelial injury in HUVECs
383 [20]. On the other hand, thrombin is a potent modulator of endothelial function, and
384 thrombin-dependent adhesion of monocytes to endothelial cells requires an intact endothelial
385 CARMA3·Bcl10·MALT1 signalosome [17], and up-regulation of PAR-1 is critically involved in
386 the co-activation of coagulation and inflammatory responses caused by thrombin [14]. In the
387 present study, co-treatment with high glucose and a thrombin inhibitor argatroban or a PAR-1
388 antagonist vorapaxar reversed the increases in NLRP1, cleaved-caspase 1, IL-18, and IL-1β levels
389 in HG-cultured HUVECs. Moreover, NLRP1 and IL-18 were markedly decreased in HUVECs
390 cultured with HG after PAR-1 knockdown by using F2R shRNA. These results demonstrated that
391 the activated NLRP1 inflammasome was due to activation of the thrombin/PAR-1 pathway in
392 endothelial cells in GDM condition.

393 AGEs may prime pro-inflammatory mechanisms through RAGE in endothelial cells, thereby
394 amplifying pro-inflammatory mechanisms in chronic inflammatory disorders [34]. RAGE
395 expression was significantly increased in the omental adipose tissue explant from GDM subjects,
396 and its ligand high mobility group box 1 protein was markedly elevated in fetal membranes from
397 GDM subjects [35]. Our finding showed that AGEs levels and RAGE protein expression were

Journal Pre-proofs

398 remarkably raised in the umbilical cord of GDM patients. Coincidentally, Tang et al. found that
399 AGEs/RAGE axis was activated in the rat model of GDM, and secretory RAGE showed a
400 protective effect on fetal development [36]. Furthermore, our cell experiments demonstrated that
401 AGEs/RAGE axis was similarly activated in HG-cultured HUVECs, and Rajaraman et al. reported
402 that HG caused vascular inflammation through AGEs mediated multiple axes besides
403 AGEs/RAGE axis in the primary culture of HUVECs [37]. These studies reinforce the enhanced
404 AGEs/RAGE interaction in vascular endothelium in chronic high glucose exposure.
405 Importantly, our observations showed that AGEs inhibition or RAGE antagonism markedly
406 decreased PAR-1 protein expression (Fig. 8A) in HG-cultured HUVECs, but did not affect
407 thrombin activity (Fig. 8B), exhibiting that the enhanced AGE/RAGE interaction mediated
408 HG-induced PAR-1 up-regulation in HUVECs. On the other hand, thrombin inhibition or PAR-1
409 antagonism significantly declined not only AGEs levels (Fig. 5A) but also RAGE protein
410 expression in HG-cultured HUVECs (Fig. 5B). Additionally, Ishibashi et al. reported that AGEs
411 potentiated the citrated plasma-induced oxidative and inflammatory reactions in endothelial cells
412 via the activation of thrombin/PAR-1 system, and blockade of the crosstalk between AGEs/RAGE
413 axis and coagulation system might be a novel therapeutic target for thromboembolic disorders in
414 diabetes [16]. In short, these results revealed an interaction between AGE/RAGE axis and
415 thrombin/PAR-1 pathway in endothelial injuries in prolonged high glucose condition.
416 The present study also testified that a natural compound Sar had an ameliorative effect on
417 endothelial damages against chronic high glucose. Timosaponin BII and AIII, the natural
418 glycosides of Sar, possess strong antiplatelet and antithrombotic effects [21, 22]. Our study
419 indicated that Sar could inhibit the activation of thrombin/PAR-1 pathway in HG-cultured

HUVECs, which may be the reasons for the antiplatelet and antithrombotic effects of the glycosides of Sar. Moreover, timosaponin BII, AIII, and Sar show powerful anti-inflammatory actions mainly through inhibiting NF-kappaB signal pathway and MAPK pathway [23-26]. In the current study, we found that Sar remarkably suppressed the activated NLRP1 inflammasome in HG-cultured HUVECs, which further clarified the action mechanism of anti-inflammatory efficacy of Sar and its glycosides. Meanwhile, our results indicated that Sar significantly inhibited AGEs/RAGE interaction in HG-cultured HUVECs. In addition, our previous report demonstrated that Sar restrained the activation of AGEs/RAGE axis in the kidney of rats with diabetic nephropathy [27]. Therefore, these findings indicated that Sar showed good protection against chronic high glucose-induced endothelial damages through several pathways, suggesting Sar a multi-target compound.

In summary, our findings demonstrated that high glucose-induced endothelial damage in GDM was associated with thrombin/PAR-1 pathway mediated activation of the NLRP1 inflammasome, and there may be an interaction between thrombin/PAR-1 pathway and AGEs/RAGE axis in endothelial damages in high glucose state (Fig. 11). Moreover, Sar could act as a multi-target protective agent against endothelial injury in prolonged HG condition (Fig. 11).

Conflict of interest

The authors declare no conflict of interest.

Acknowledgements

The work was supported through funding from Qing Lan Project of Jiangsu Province (2014), China, and Fundamental Research Funds for the Research on Graduate Innovation Program,

Jiangsu Province (NO: KYCX17_1731), China.

References

[1] H.S.C.R. Group, B.E. Metzger, L.P. Lowe, A.R. Dyer, E.R. Trimble, U. Chaovarindr, D.R. Coustan, D.R. Hadden, D.R. McCance, M. Hod, H.D. McIntyre, J.J. Oats, B. Persson, M.S. Rogers, D.A. Sacks, Hyperglycemia and adverse pregnancy outcomes, N Engl J Med 358(19) (2008) 1991-2002.

[2] D. Dabelea, D.J. Pettitt, Intrauterine diabetic environment confers risks for type 2 diabetes mellitus and obesity in the offspring, in addition to genetic susceptibility, J Pediatr Endocrinol Metab 14(8) (2001) 1085-91.

[3] L. Bellamy, J.P. Casas, A.D. Hingorani, D. Williams, Type 2 diabetes mellitus after gestational diabetes: a systematic review and meta-analysis, Lancet 373(9677) (2009) 1773-9.

[4] D. Katz, Y. Beilin, Disorders of coagulation in pregnancy, Br J Anaesth 115 Suppl 2 (2015) ii75-88.

[5] L. Pretorius, G.J.A. Thomson, R.C.M. Adams, T.A. Nell, W.A. Laubscher, E. Pretorius, Platelet activity and hypercoagulation in type 2 diabetes, Cardiovasc Diabetol 17(1) (2018) 141.

[6] J. Bendl, J. Kvasnicka, A. Umlaufova, J. Kvasnicka, Jr., J. Zivny, [Hemostasis and levels of cytoadhesion molecules in gestational diabetes], Ceska Gynekol 64(2) (1999) 83-6.

[7] Gumus, II, A. Kargili, F. Karakurt, B. Kasapoglu, A. Derbent, I. Kaygusuz, C. Koca, S. Sevgili, Levels of thrombin activatable fibrinolysis inhibitor in gestational diabetes mellitus, Gynecol Endocrinol 29(4) (2013) 327-30.

[8] S.R. Coughlin, Thrombin signalling and protease-activated receptors, Nature 407(6801) (2000)

258-64.

[9] H.S. Bajaj, C. Ye, A.J. Hanley, M. Sermer, B. Zinman, R. Retnakaran, Biomarkers of vascular injury and endothelial dysfunction after recent glucose intolerance in pregnancy, Diab Vasc Dis Res 15(5) (2018) 449-457.

[10] M.D. Savvidou, L. Geerts, K.H. Nicolaides, Impaired vascular reactivity in pregnant women with insulin-dependent diabetes mellitus, Am J Obstet Gynecol 186(1) (2002) 84-8.

[11] P. Pantham, I.L. Aye, T.L. Powell, Inflammation in maternal obesity and gestational diabetes mellitus, Placenta 36(7) (2015) 709-15.

[12] N. Zheng, X. Shi, X. Chen, W. Lv, Associations Between Inflammatory Markers, Hemostatic Markers, and Microvascular Complications in 182 Chinese Patients With Type 2 Diabetes Mellitus, Lab Med 46(3) (2015) 214-20.

[13] W.M. Cheung, M.R. D'Andrea, P. Andrade-Gordon, B.P. Damiano, Altered vascular injury responses in mice deficient in protease-activated receptor-1, Arterioscler Thromb Vasc Biol 19(12) (1999) 3014-24.

[14] C. Schoergenhofer, M. Schwameis, G. Gelbenegger, N. Buchtele, B. Thaler, M. Mussbacher, G. Schabbauer, J. Wojta, P. Jilma-Stohlawetz, B. Jilma, Inhibition of Protease-Activated Receptor (PAR1) Reduces Activation of the Endothelium, Coagulation, Fibrinolysis and Inflammation during Human Endotoxemia, Thromb Haemost 118(7) (2018) 1176-1184.

[15] K. De Ceunynck, C.G. Peters, A. Jain, S.J. Higgins, O. Aisiku, J.L. Fitch-Tewfik, S.A. Chaudhry, C. Dockendorff, S.M. Parikh, D.E. Ingber, R. Flaumenhaft, PAR1 agonists stimulate APC-like endothelial cytoprotection and confer resistance to thromboinflammatory injury, Proc Natl Acad Sci U S A 115(5) (2018) E982-E991.

[16] Y. Ishibashi, T. Matsui, S. Ueda, K. Fukami, S. Yamagishi, Advanced glycation end products potentiate citrated plasma-evoked oxidative and inflammatory reactions in endothelial cells by up-regulating protease-activated receptor-1 expression, Cardiovasc Diabetol 13 (2014) 60.

[17] P.C. Delekta, I.J. Apel, S. Gu, K. Siu, Y. Hattori, L.M. McAllister-Lucas, P.C. Lucas, Thrombin-dependent NF-{kappa}B activation and monocyte/endothelial adhesion are mediated by the CARMA3.Bcl10.MALT1 signalosome, J Biol Chem 285(53) (2010) 41432-42.

[18] K. Tantivejkul, R.D. Loberg, S.C. Mawocha, L.L. Day, L.S. John, B.A. Pienta, M.A. Rubin, K.J. Pienta, PAR1-mediated NFkappaB activation promotes survival of prostate cancer cells through a Bcl-xL-dependent mechanism, J Cell Biochem 96(3) (2005) 641-52.

[19] P.R. Lee, T.P. Johnson, S. Gnanapavan, G. Giovannoni, T. Wang, J.P. Steiner, M. Medynets, M.J. Vaal, V. Gartner, A. Nath, Protease-activated receptor-1 activation by granzyme B causes neurotoxicity that is augmented by interleukin-1beta, J Neuroinflammation 14(1) (2017) 131.

[20] T. Jiang, D. Jiang, L. Zhang, M. Ding, H. Zhou, Anagliptin ameliorates high glucose-induced endothelial dysfunction via suppression of NLRP3 inflammasome activation mediated by SIRT1, Mol Immunol 107 (2019) 54-60.

[21] Z.-H.Z. Su-Yan Li, Hai-Yun Pei, et al. , Effect of timosaponin AⅢ on formation of thrombus, Bull Acad Mil Med Sci 30(4) (2006) 340-342.

[22] W.Q. Lu, Y. Qiu, T.J. Li, X. Tao, L.N. Sun, W.S. Chen, Antiplatelet and antithrombotic activities of timosaponin B-II, an extract of Anemarrhena asphodeloides, Clin Exp Pharmacol Physiol 38(7) (2011) 430-4.

[23] Z. Wang, J. Cai, Q. Fu, L. Cheng, L. Wu, W. Zhang, Y. Zhang, Y. Jin, C. Zhang,

508 Anti-Inflammatory Activities of Compounds Isolated from the Rhizome of Anemarrhena
509 asphodeloides, Molecules 23(10) (2018).
510 [24] W.Q. Lu, Y. Qiu, T.J. Li, X. Tao, L.N. Sun, W.S. Chen, Timosaponin B-II inhibits
511 pro-inflammatory cytokine induction by lipopolysaccharide in BV2 cells, Arch Pharm Res
512 32(9) (2009) 1301-8.
513 [25] J.Y. Kim, J.S. Shin, J.H. Ryu, S.Y. Kim, Y.W. Cho, J.H. Choi, K.T. Lee, Anti-inflammatory
514 effect of anemarsaponin B isolated from the rhizomes of Anemarrhena asphodeloides in
515 LPS-induced RAW 264.7 macrophages is mediated by negative regulation of the nuclear
516 factor-kappaB and p38 pathways, Food Chem Toxicol 47(7) (2009) 1610-7.
517 [26] S.M. Lim, J.J. Jeong, G.D. Kang, K.A. Kim, H.S. Choi, D.H. Kim, Timosaponin AIII and its
518 metabolite sarsasapogenin ameliorate colitis in mice by inhibiting NF-kappaB and MAPK
519 activation and restoring Th17/Treg cell balance, Int Immunopharmacol 25(2) (2015) 493-503.
520 [27] Y.W. Liu, Y.C. Hao, Y.J. Chen, S.Y. Yin, M.Y. Zhang, L. Kong, T.Y. Wang, Protective
521 effects of sarsasapogenin against early stage of diabetic nephropathy in rats, Phytother Res
522 32(8) (2018) 1574-1582.
523 [28] D. International Association of, P. Pregnancy Study Groups Consensus, B.E. Metzger, S.G.
524 Gabbe, B. Persson, T.A. Buchanan, P.A. Catalano, P. Damm, A.R. Dyer, A. Leiva, M. Hod,
525 J.L. Kitzmiler, L.P. Lowe, H.D. McIntyre, J.J. Oats, Y. Omori, M.I. Schmidt, International
526 association of diabetes and pregnancy study groups recommendations on the diagnosis and
527 classification of hyperglycemia in pregnancy, Diabetes Care 33(3) (2010) 676-82.
528 [29] D. Lei, L. Chengcheng, Q. Xuan, C. Yibing, W. Lei, Y. Hao, L. Xizhi, L. Yuan, Y. Xiaoxing,
529 L. Qian, Quercetin inhibited mesangial cell proliferation of early diabetic nephropathy through

Journal Pre-proofs

the Hippo pathway, Pharmacol Res 146 (2019) 104320.

[30] L. Bao, J. Zu, Q. He, H. Zhao, S. Zhou, X. Ye, X. Yang, K. Zan, Z. Zhang, H. Shi, G. Cui, Thrombin-induced apoptosis in neurons through activation of c-Jun-N-terminal kinase, Toxicol Mech Methods 27(1) (2017) 18-23.

[31] D. Bushi, J. Chapman, A. Katzav, E. Shavit-Stein, N. Molshatzki, N. Maggio, D. Tanne, Quantitative detection of thrombin activity in an ischemic stroke model, J Mol Neurosci 51(3) (2013) 844-50.

[32] L. Du, L. Wang, B. Wang, J. Wang, M. Hao, Y.B. Chen, X.Z. Li, Y. Li, Y.F. Jiang, C.C. Li, H. Yang, X.K. Gu, X.X. Yin, Q. Lu, A novel compound AB38b attenuates oxidative stress and ECM protein accumulation in kidneys of diabetic mice through modulation of Keap1/Nrf2 signaling, Acta pharmacologica Sinica (2019).

[33] P. Bortolotti, E. Faure, E. Kipnis, Inflammasomes in Tissue Damages and Immune Disorders After Trauma, Front Immunol 9 (2018) 1900.

[34] G. Basta, G. Lazzerini, M. Massaro, T. Simoncini, P. Tanganelli, C. Fu, T. Kislinger, D.M. Stern, A.M. Schmidt, R. De Caterina, Advanced glycation end products activate endothelium through signal-transduction receptor RAGE: a mechanism for amplification of inflammatory responses, Circulation 105(7) (2002) 816-22.

[35] C. Santangelo, T. Filardi, G. Perrone, M. Mariani, E. Mari, B. Scazzocchio, R. Masella, R. Brunelli, A. Lenzi, A. Zicari, S. Morano, Cross-talk between fetal membranes and visceral adipose tissue involves HMGB1-RAGE and VIP-VPAC2 pathways in human gestational diabetes mellitus, Acta Diabetol 56(6) (2019) 681-689.

[36] X. Tang, Q. Qin, X. Xie, P. He, Protective effect of sRAGE on fetal development in pregnant

552 rats with gestational diabetes mellitus, Cell Biochem Biophys 71(2) (2015) 549-56.

553 [37] B. Rajaraman, N. Ramadas, S. Krishnasamy, V. Ravi, A. Pathak, C.S. Devasena, K.

554 Swaminathan, A. Ganeshprasad, A.A. Kuppuswamy, S. Vedantham, Hyperglycaemia cause

555 vascular inflammation through advanced glycation end products/early growth response-1 axis

556 in gestational diabetes mellitus, Mol Cell Biochem 456(1-2) (2019) 179-190.

557

Journal Pre-proofs

559 **Figure captions**

560 **Fig. 1** Thrombin activity (A), PAR-1 expression (B), RAGE expression (C), and AGEs levels (D)
561 in the umbilical cord of GDM patients. The 60-70 μg protein was loaded onto the gel in Western
562 blot detection. Mean ± SEM, thrombin (n=8), PAR-1 (n=6), RAGE (n=6). **P<0.01, compared
563 with N. Scale bar: 20 μm.

564

565 **Fig. 2** Protein expressions of NLRP1 (A) and cleaved caspase-1 (B) in umbilical cord, and IL-18
566 levels in plasma (C) of GDM patients. The 60-70 μg protein was loaded onto the gel in Western
567 blot detection. Mean ± SEM, NLRP1 and cleaved caspase-1 (n=6), IL-18 (n=31-32). *P<0.05,
568 **P<0.01, compared with N.

569

570 **Fig. 3** Protein expression of PAR-1 in HUVECs cultured with high glucose for 24 h, 48 h, and 72
571 h by immunofluorescence. NG and HG represented 5.6 mmol/L glucose and 30 mmol/L glucose,
572 respectively. Scale bar: 20 μm.

573

574 **Fig. 4** Effects of sarsasapogenin (Sar) on thrombin activity (A) and PAR-1 expression (B) in
575 HUVECs cultured with high glucose for 48 h. NG, HG, HG+Sar-0.2, HG+Sar-1, HG+Sar-5,
576 HG+Vor, and HG+Arg groups: cells treated with 5.6 mmol/L glucose, 30 mmol/L glucose, 30
577 mmol/L glucose plus 0.2, 1, 5 μmol/L Sar, 1.0 μmol/L vorapaxar (Vor, a selective PAR-1
578 antagonist), or 1.0 μmol/L argatroban (Arg, a typical inhibitor of thrombin), respectively. The 50
579 μg protein was loaded onto the gel in Western blot detection. Mean ± SEM, thrombin (n=6),
580 PAR-1 (n=3). *P<0.05, compared with NG; $^{\#}P$<0.05, $^{\#\#}P$<0.01, compared with HG.

Journal Pre-proofs

Fig. 5 Effects of sarsasapogenin (Sar) on AGEs levels (A) and protein expression of RAGE (B) in HUVECs treated with high glucose for 48 h. NG, HG, HG+Sar-0.2, HG+Sar-1, HG+Sar-5, HG+Vor, and HG+Arg groups: cells treated with 5.6 mmol/L glucose, 30 mmol/L glucose, 30 mmol/L glucose plus 0.2, 1, 5 μmol/L Sar, 1.0 μmol/L vorapaxar (Vor, a selective PAR-1 antagonist), or 1.0 μmol/L argatroban (Arg, a typical inhibitor of thrombin), respectively. The 50 μg protein was loaded onto the gel in Western blot detection. Mean ± SEM, RAGE (n=3). $^{**}P < 0.01$, compared with NG; $^{\#}P<0.05$, $^{\#\#}P<0.01$, compared with HG.

Fig. 6 Effects of sarsasapogenin (Sar) on cell viability (A) and LDH release (B) in HUVECs cultured with high glucose for 48 h. NG, HG, HG+Sar-0.2, HG+Sar-1, HG+Sar-5, HG+Vor, and HG+Arg groups: cells treated with 5.6 mmol/L glucose, 30 mmol/L glucose, 30 mmol/L glucose plus 0.2, 1, 5 μmol/L Sar, 1.0 μmol/L vorapaxar (Vor, a selective PAR-1 antagonist), or 1.0 μmol/L argatroban (Arg, a typical inhibitor of thrombin), respectively. Mean ± SEM, n=3. $^{*}P<0.05$, $^{**}P<0.01$, compared with NG; $^{\#}P<0.05$, $^{\#\#}P<0.01$, compared with HG.

Fig. 7 Effects of sarsasapogenin (Sar) on protein expressions of NLRP1 (A), cleaved caspase-1 (B), IL-18 (C), and IL-1β (D) in HUVECs treated with high glucose for 48 h. NG, HG, HG+Sar-0.2, HG+Sar-1, HG+Sar-5, HG+Vor, and HG+Arg groups: cells treated with 5.6 mmol/L glucose, 30 mmol/L glucose, 30 mmol/L glucose plus 0.2, 1, 5 μmol/L Sar, 1.0 μmol/L vorapaxar (Vor, a selective PAR-1 antagonist), or 1.0 μmol/L argatroban (Arg, a typical inhibitor of thrombin), respectively. The 50 μg protein was loaded onto the gel in Western blot detection.

603 Mean ± SEM, NLRP1 (n=5), cleaved caspase-1 (n=4), IL-18 and IL 1β (n=3). *P < 0.05, **P <
604 0.01, compared with NG; $^{\#}P$<0.05, $^{\#\#}P$<0.01, compared with HG.
605
606 **Fig. 8** Effects of inhibition of AGEs/RAGE axis on PAR-1 expression (A) and thrombin activity
607 (B) in HUVECs cultured with high glucose for 48 h. HG, HG+Sar-5, HG+AG, and HG+FPS-ZM1
608 groups represent cells treated with 30 mmol/L glucose, 30 mmol/L glucose plus 5 μmol/L Sar, 1
609 μmol/L aminoguanidine (AG, a typical inhibitor of AGEs formation), or 1 μmol/L FPS-ZM1 (a
610 high-affinity inhibitor of RAGE), respectively. The 50 μg protein was loaded onto the gel in
611 Western blot detection. Mean ± SEM, PAR-1 (n=5), thrombin (n=6). *P<0.05, **P<0.01,
612 compared with HG.
613
614 **Fig. 9** Interference efficiency of F2R shRNA (shF2R) was performed in HUVECs. (A) HUVECs
615 infected with lentivirus containing F2R shRNA (F2R as the gene symbol of PAR-1) under
616 bright-field microscopy illumination, and fluorescent light in the same field showed stable and
617 high expression of green fluorescent protein (GFP). (B) The protein levels of PAR-1 by Western
618 blot using 50 μg total proteins. Mean ± SEM, n=3, **P<0.01, compared with vehicle (shNC).
619
620 **Fig. 10** Effects of PAR-1 knockdown on protein expressions of NLRP1 (A) and IL-18 (B) in
621 HUVECs treated with high glucose for 48 h. HG, HG+Sar-5, shF2R+HG, and shF2R+HG+Sar-5
622 groups represent cells infected with lentivirus containing F2R negative control (shNC) or F2R
623 shRNA (F2R, the gene symbol of PAR-1) subsequently cultured with HG or HG plus 5 μmol/L
624 Sar, respectively. The 50 μg protein was loaded onto the gel in Western blot detection. Mean ±

Journal Pre-proofs

SEM, NLRP1 (n=3), IL-18 (n=5). $^{**}P < 0.01$, compared with HG; $^{\#}P<0.05$, $^{\#\#}P<0.01$, compared with HG+Sar-5.

Credit Author Statement

Liu Yao-Wu: Conceptualization, Project administration, Funding acquisition, Writing-Review & Editing. **Liu Yue:** Investigation, Methodology, Data curation, Writing-Original draft preparation**. Tang Zhuang-Zhuang:** Methodology, Validation, Data curation. **Zhang Yu-Meng:** Resources, Visualization. **Kong Li:** Methodology, Funding acquisition. **Xiao Wei-Fen:** Conceptualization, Supervision. **Ma Teng-Fei:** Visualization, Writing- Reviewing and Editing.

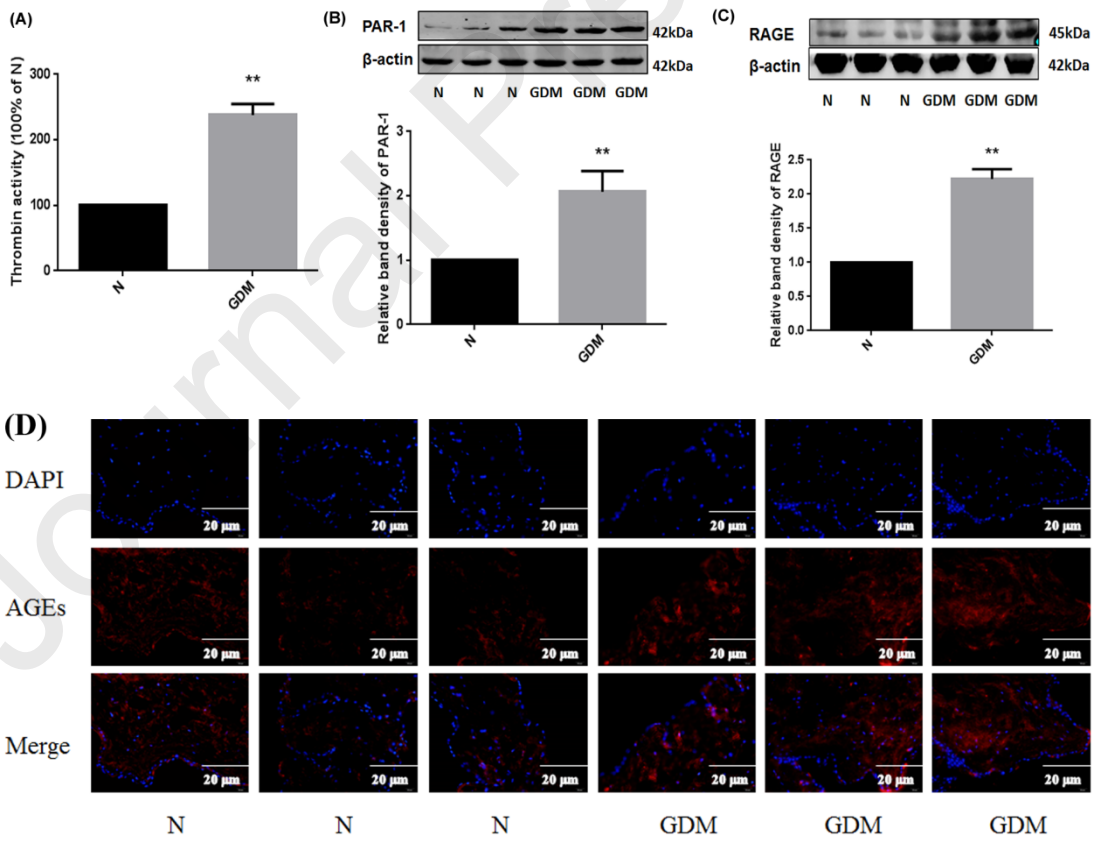

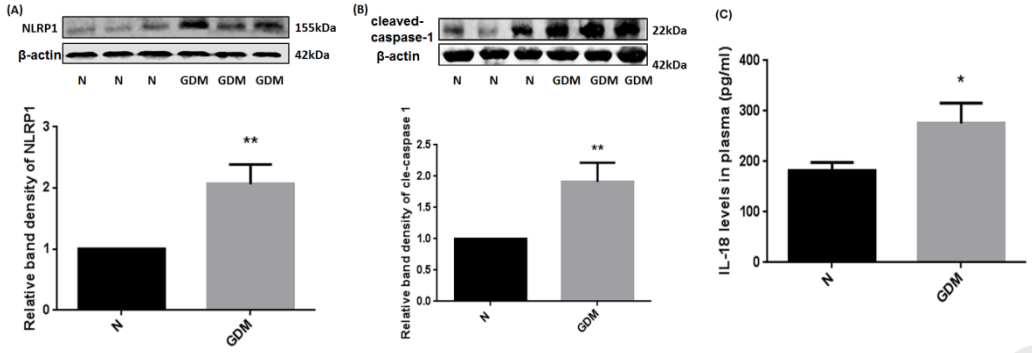
(A)
NLRP1
155kDa
β-actin
42kDa
N N N GDM GDM GDM
Relative band density of NLRP1
**
N
GDM
(B)
cleaved-caspase-1
22kDa
β-actin
42kDa
N N N GDM GDM GDM
Relative band density of cle-caspase 1
**
N
GDM
(C)
IL-18 levels in plasma (pg/ml)
*
N
GDM

637

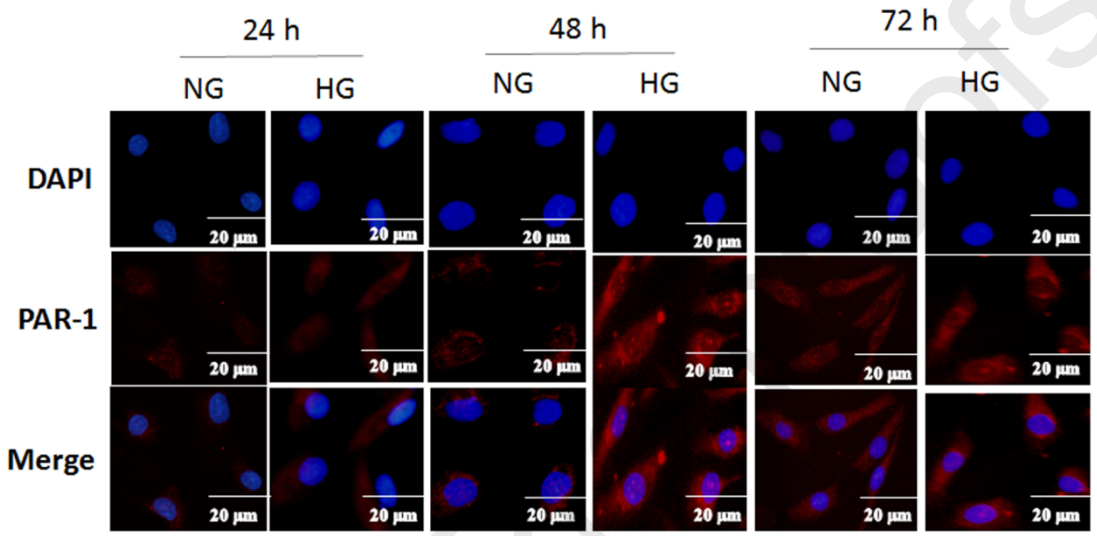
24 h
48 h
72 h
NG
HG
NG
HG
NG
HG
DAPI
PAR-1
Merge
20 μm

638

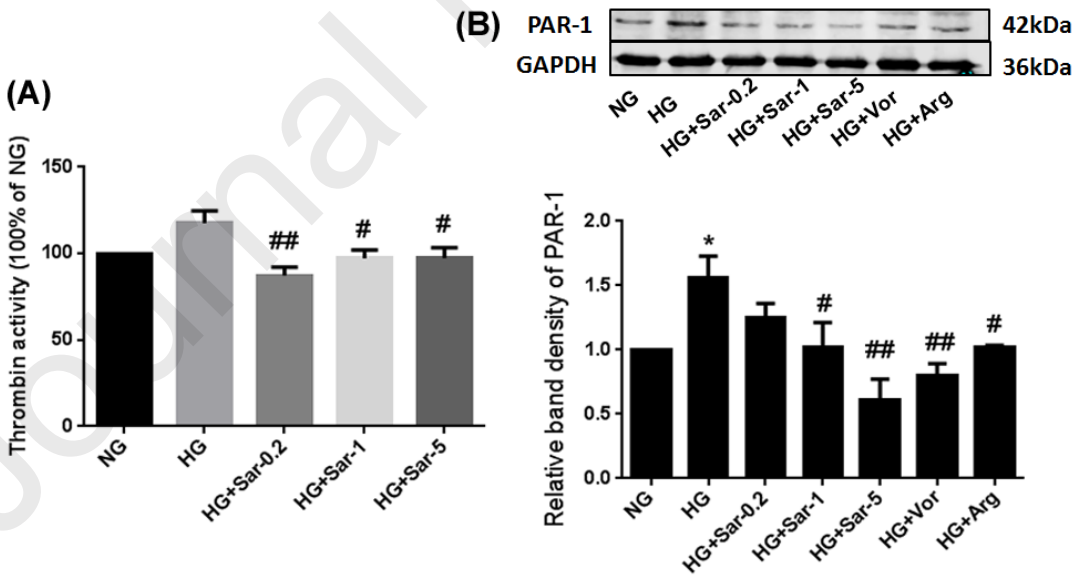
(A)
Thrombin activity (100% of NG)
NG
HG
HG+Sar-0.2
HG+Sar-1
HG+Sar-5
##
#
#
(B)
PAR-1
42kDa
GAPDH
36kDa
NG
HG
HG+Sar-0.2
HG+Sar-1
HG+Sar-5
HG+Vor
HG+Arg
Relative band density of PAR-1
*
#
##
##
#

639

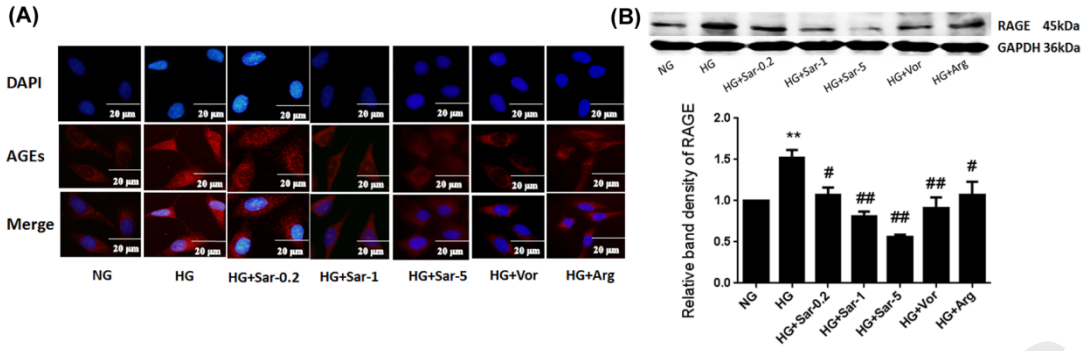

640

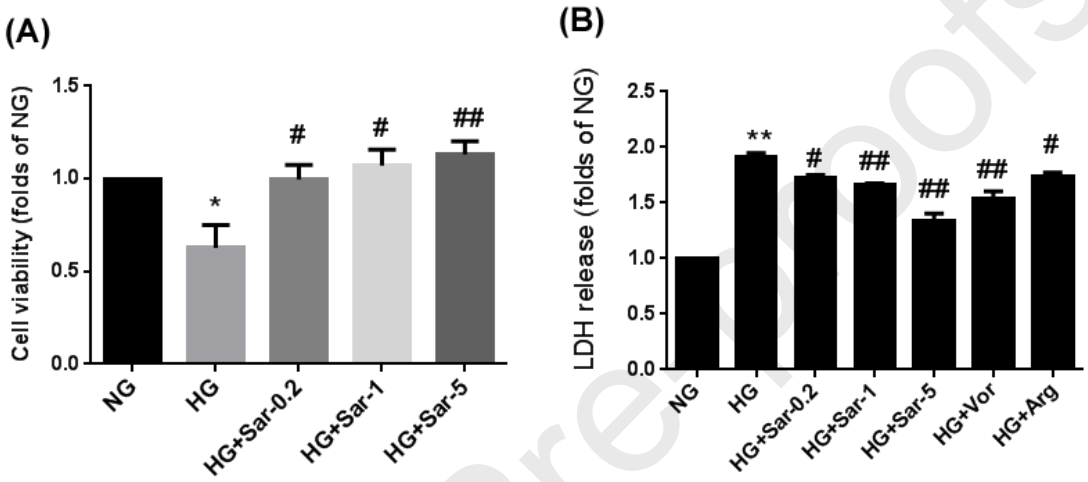

641

Journal Pre-proofs

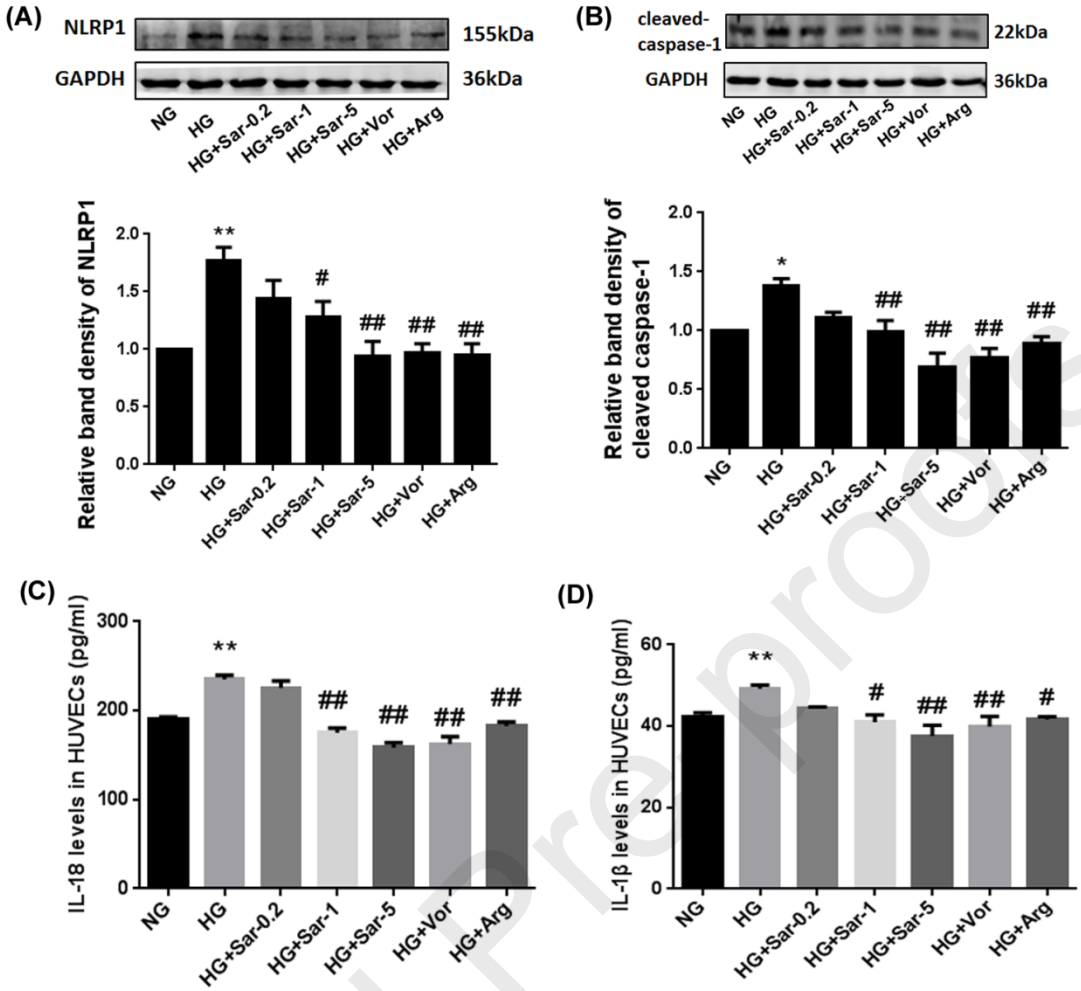

642

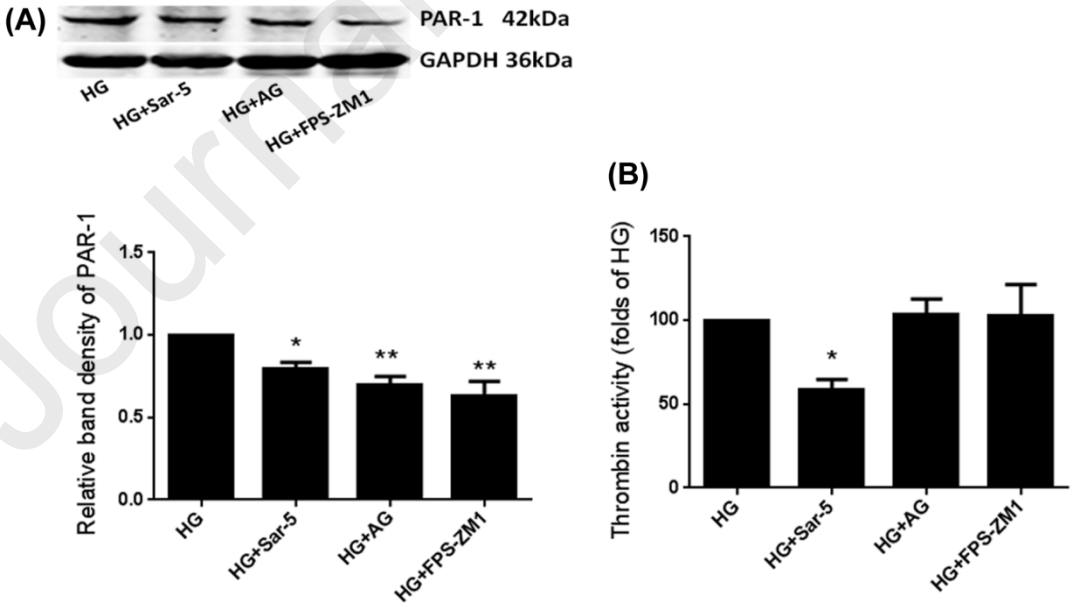

643

Journal Pre-proofs

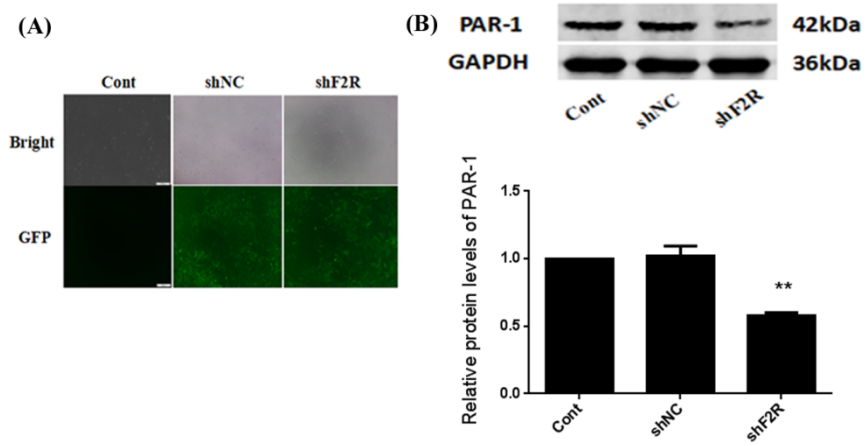

644

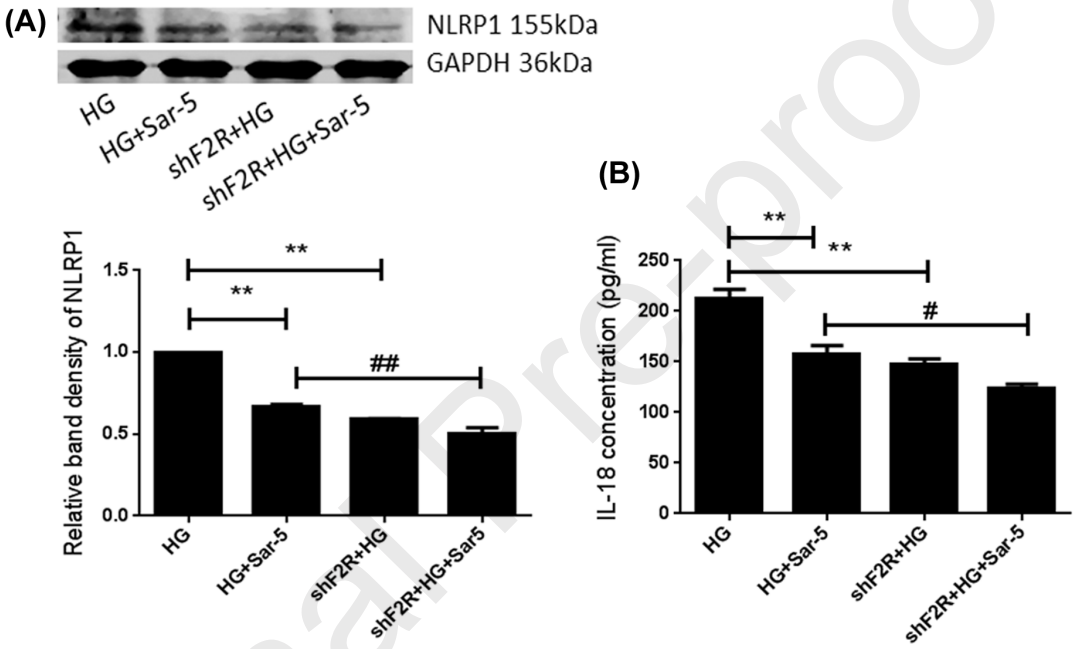

645

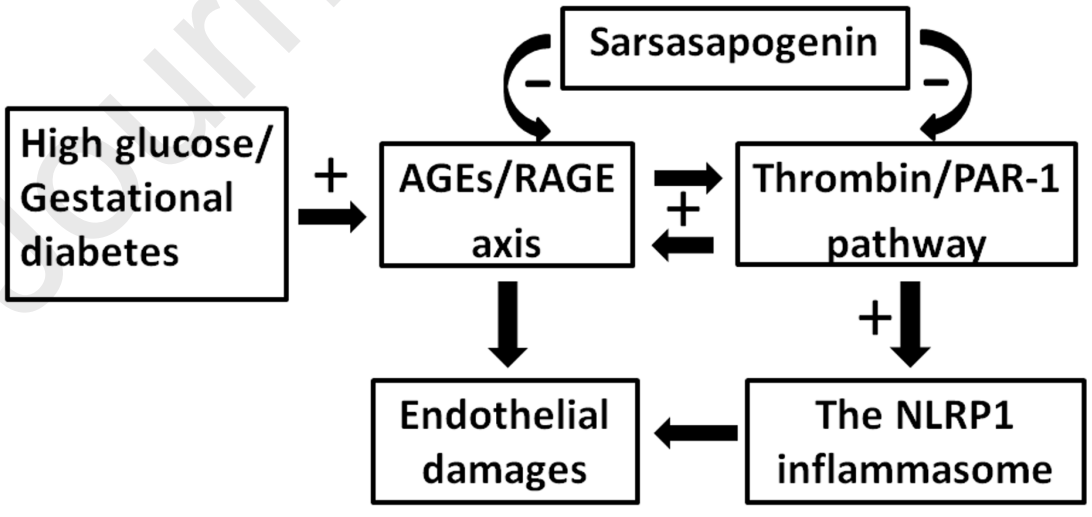

646

Journal Pre-proofs

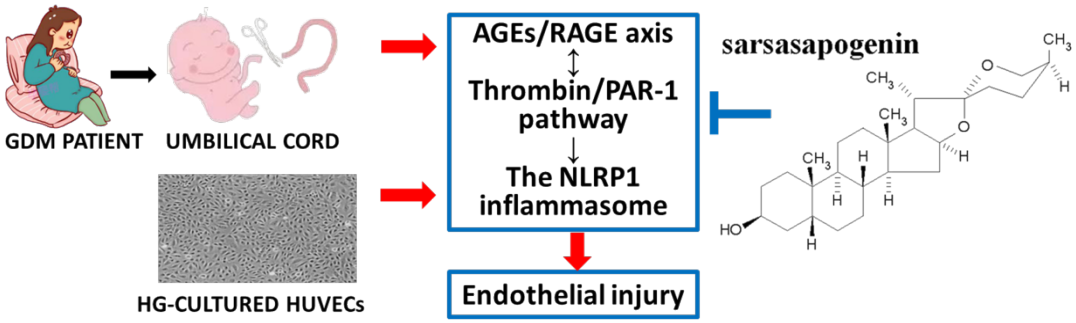

647

Journal Pre-proofs